Peptide Binding in OppA, the Crystal Structures of the Periplasmic Oligopeptide Binding Protein in the Unliganded Form and in Complex with Lysyllysine[†,‡]

Sara H. Sleigh, Jeremy R. H. Tame,[§] Eleanor J. Dodson,[||] and Anthony J. Wilkinson*

Department of Chemistry, University of York, York Y01 5DD, U.K.

Received February 27, 1997; Revised Manuscript Received May 28, 1997[⊗]

ABSTRACT: The periplasmic oligopeptide binding protein, OppA, acts as the initial receptor for the uptake of peptides by the oligopeptide permease (Opp) in Gram-negative bacteria. Opp will handle peptides between two and five amino acid residues regardless of their sequence. The crystal structures of a series of OppA−peptide complexes have revealed an enclosed but versatile peptide binding pocket and have illustrated how tri- and tetrapeptide ligands are accommodated. Here, the crystal structures of (i) OppA complexed with a dipeptide (lysyllysine) and (ii) unliganded OppA have been solved using X-ray data extending to 1.8 and 2.4 Å spacing, respectively. In the dipeptide complex, the α-amino group of the ligand is anchored through an ion pair interaction with Asp^{419}, as observed in complexes with longer peptides. However, its α-carboxylate group forms water-mediated interactions with the guanidinium groups of Arg^{404} and Arg^{413} rather than the direct salt bridges to Arg^{413} and His^{371} observed in the tripeptide and tetrapeptide complexes, respectively. Isothermal titration calorimetric measurements of the binding of lysine-containing peptides of different lengths to OppA show that the dipeptide, KK, is bound with ∼60-fold lower affinity than related tri- and tetrapeptides (KKK and KKKA, respectively). These data are discussed with reference to the calculated enthalpic and entropic contributions to ligand binding and the structures of the OppA peptide complexes. In the unliganded molecule, domain III has rotated as a rigid body through 26° away from domains I and II, exposing the ligand binding site. The water structure in the binding cleft shows similarities to that in the various OppA−peptide complexes.

The periplasmic binding protein dependent permeases constitute a large and important class of active transport systems for the uptake of sugars, amino acids, anions, peptides, and other nutrients by Gram-negative bacteria (Ames, 1986; Furlong, 1987; Higgins, 1992). These transporters share a common organization, each comprising two integral membrane components which form a channel through which the solute passes, together with two components at the cytoplasmic surface of the membrane which couple ATP hydrolysis to solute translocation (Higgins *et al.*, 1982). The fifth component is a soluble periplasmic protein which acts as the receptor, capturing substrates in the periplasm and delivering them to the membrane components for transport. These periplasmic substrate binding proteins largely define the specificity of their respective transport systems and therefore have a key role in governing the range of molecules that may enter a cell.

Extensive crystallographic analysis has shown that the periplasmic receptors are closely related in structure even though they lack significant sequence similarity and recognize diverse ligands (Quiocho & Ledvina, 1996). Each contains two globular domains connected by short segments of polypeptide chain which act as a hinge, allowing relative domain movements to take place. The ligand binds in a deep cleft formed between the two domains which close around the substrate, in a manner reminiscent of a "Venus fly trap" (Mao *et al.*, 1982). Sequestration of ligands in this way is inevitably associated with abundant receptor−substrate interactions allowing the binding proteins to impose selectivity on their ligands. These crystal structures have provided explanations for the often subtle substrate specificities of particular proteins, as well as providing chemical insights into the wider field of molecular recognition. For example, the periplasmic binding proteins associated with the sulfate (SBP)[1] and phosphate (PBP) transporters bind sulfate and phosphate anions, respectively, with high affinity while efficiently discriminating against the noncognate ion. The arrangement of hydrogen bond donor and acceptor groups in the respective binding sites imposes discrimination on the basis of the different charges and/or protonation states of sulfate and phosphate ions and also accounts for the capacity of SBP to bind selenate and PBP to bind arsenate (Jacobson & Quiocho, 1988; Luecke & Quiocho, 1990). In sugar transport, the anomeric and epimeric tolerances of arabinose binding protein (ABP) and glucose/galactose binding protein (GGBP) have been attributed to the presence in the binding pockets of strategically positioned aspartate side chains which are able to form charge−dipole interactions with the C_1 hydroxyl group of α- and β-arabinose or the C_4 hydroxyl groups of glucose and galactose, respectively (Quiocho & Vyas, 1984; Quiocho *et al.*, 1989, Vyas *et al.*, 1994). The capacity of lysine/arginine/ornithine binding protein (LAOBP) to bind the basic side chains of its different sized ligands is achieved through alternative arrangements of a protein

[†] This work was supported by Biotechnology and Biological Sciences Research Council, U.K., Grant GR/H68864.

[‡] Brookhaven PDB codes: 1RKM, unliganded OppA; 2RKM, OppA−KK complex.

[§] Royal Society University Research Fellow.

[||] Supported by the Medical Research Council.

[⊗] Abstract published in *Advance ACS Abstracts,* July 15, 1997.

[1] Abbreviations: OppA, oligopepetide binding protein; ITC, isothermal titration calorimetry; SBP, sulfate binding protein; PBP, phosphate binding protein; ABP, arabinose binding protein; GGBP, glucose/galactose binding protein; LAOBP, lysine/arginine/ornithine binding protein; DppA, dipepetide binding protein; MBP, maltodextrin binding protein; LIVBP, leucine/isoleucine/valine binding protein.

S0006-2960(97)00457-1 CCC: $14.00

carboxylate group and nearby water molecules in the amino acid binding cavity (Oh *et al*., 1994).

The most versatile of the periplasmic receptors are those associated with the dipeptide (Dpp) and oligopeptide (Opp) permeases (Abouhamad *et al.*, 1991; Higgins *et al.*, 1982). Peptides can act as the sole source of carbon and nitrogen for the growth of enteric bacteria, such as *Escherichia coli* and *Salmonella typhimurium*, and their peptide transporters have evolved broad specificities to handle the enormous potential chemical variety of short peptides found in the surrounding medium. The specificity of the oligopeptide permease has been defined predominantly through genetic experiments which illustrated that amino acid auxotrophic strains of *E. coli* can use oligopeptides as a source of the required amino acid. Substrains selected for their resistance to the toxic peptide triornithine were shown to have lost the ability to grow on a range of oligopeptides that were otherwise nutritionally active (Payne & Gilvarg, 1968; Payne, 1968). These studies led to the conclusion that the oligopeptide permease can handle peptides two to five amino acid residues in length with little regard to their sequence. The critical requirements appeared to be a positively charged N-terminus and an unmodified α-peptide linkage. Equilibrium dialysis experiments subsequently examined the capacity of defined peptides to compete with Ala-Phe-[^{3}H]Gly on binding to the oligopeptide binding protein, OppA. This confirmed that the specificity of OppA correlates with the specificity of the transport system and, in addition, showed that dipeptides and pentapeptides competed much less efficiently than the tripeptides and tetrapeptides examined (Guyer *et al*., 1986).

To explore the structural basis of sequence-independent peptide binding in OppA, we have determined the crystal structure of OppA in complex with tripeptide and tetrapeptide ligands (Tame *et al.*, 1994, 1995). The ligands are completely enclosed in the protein interior with specific interactions being made between the peptide main chain and the protein. The amino termini of both tri- and tetrapeptide ligands form a salt bridge with the side chain of Asp^{419}.[2] A series of positively charged protein side chains distributed at intervals along the binding cavity appear to allow the α-carboxylate groups of peptides of different lengths to make similar salt-bridging interactions with the protein. The ligand side chains, in contrast, project into spacious and hydrated pockets in which few direct contacts are made with the protein, so that side chains of differing size and charge are accommodated with minimal adjustment of the surrounding protein structure (Tame *et al.*, 1996). This method of accommodating peptides of diverse structure in a single binding pocket differs from strategies for coping with this problem adopted by other peptide binding proteins (Wilkinson, 1996).

The enclosed peptide binding pocket with its wide tolerance of ligand structures warrants further investigation. As an extension of earlier studies of the binding of tripeptide and tetrapeptide ligands, we present here the crystal structure of OppA in complex with a dipeptide together with thermodynamic data on the binding of three peptides of differing length. We have also crystallized the unliganded protein and determined its structure by molecular replacement methods in order to examine the changes in conformation and hydration that accompany ligand binding.

[2] Throughout the paper we number amino acid residues with a superscript (e.g., Ala^1) and ligand residues with a hyphen (e.g., Lys-1). In both structures described here the water molecules have been ordered by temperature factor (*B*).

Table 1: Data Collection and Refinement Statistics for the Structures of Unliganded OppA and OppA Complexed with Dilysine

	unliganded OppA	OppA−KK complex
space group	$P3_221$	$P2_12_12_1$
unit cell dimensions (Å)	$a = b = 97.84$, $c = 137.21$	$a = 110.47$, $b = 77.15$, $c = 71.59$
temp of data collection (K)	298	120
resolution limits (Å)	15−2.4	20−1.8
total no. of observations	112007	379533
no. of unique reflections	30015	57099
average multiplicity	3.7	6.6
completeness (%)		
overall	99.3	92.9
outermost resolution shell	99.5 (2.53−2.40 Å)	98.9 (1.89−1.8 Å)
R_{merge}[a] (%)		
overall	10.3	7.2
outermost resolution shell	45.7 (2.53−2.40 Å)	21.9 (1.89−1.8 Å)
mean $I/\sigma I$		
overall	6.8	7.6
outermost resolution shell	1.6 (2.53−2.40 Å)	3.4 (1.89−1.8 Å)
no. of protein atoms	4190	4209
no. of solvent atoms	125	536
R_{cryst}[a] (%)	19.1	16.7
free R_{cryst} (%)	24.7	20.2
RMS bond (Å)	0.018	0.006
RMS angle (Å)	0.049	0.022
RMS planes (Å)	0.051	0.024
av temp factors (Å^2)		
main chain	25.5	14.5
side chain	29.0	17.0
solvent	30.2	24.4

[a] $R_{merge} = \Sigma|I_i - I_n|/\Sigma I_n$, where I_i is an observed intensity *hkl* and I_n is the average of the observed equivalents. $R_{cryst} = \Sigma_{hkl}||F_o| - |F_c||/|F_o|$, where $|F_o|$ and $|F_c|$ are the magnitudes of the observed and calculated structure factor amplitudes of a reflection *hkl* respectively. All data were included in the calculation of R_{cryst} and free $R_{cryst.}$ No intensity or resolution cutoff was applied.

EXPERIMENTAL PROCEDURES

Crystallization and Data Collection. Unliganded OppA was purified as previously described (Tame *et al*., 1995) and crystallized from hanging drops containing 3 M $(NH_4)_2SO_4$, 0.3 M NaCl, and ∼30 mg/mL protein in 0.1 M HEPES buffer (pH 7.5). Small hexagonal rod-shaped crystals appeared within 1 week. The crystals grow in the trigonal space group $P3_221$. OppA−KK crystals were prepared using procedures established for OppA tripeptide complexes and crystallize in the space group $P2_12_12_1$. Crystallization solutions contained 6% poly(ethylene glycol) 4000, 1 mM uranyl acetate, and ∼25 mg/mL OppA in 50 mM sodium acetate (pH 5.5) (Tame *et al*., 1995). Both crystal lattices contain one molecule in the asymmetric unit.

X-ray diffraction data were collected from single crystals at the SRS, Daresbury, Station 9.5 using a large Mar research image plate. In the case of the OppA−KK complex, data were collected at 120 K using an Oxford Cryostream system. Data reduction and scaling were carried out using DENZO (Otwinowski, 1990) and CCP4 software (CCP4, 1994). Data collection and processing statistics are shown in Table 1.

Refinement of the OppA−KK Complex. The OppA−KK crystals are isomorphous with those of other OppA−peptide

complexes previously solved in the same space group (Glover *et al*., 1994; Tame *et al*., 1995). The OppA−KAK complex (pdb code 1jet) was used as the starting model for refinement as this structure has been solved to the highest resolution (1.2 Å). Before refinement the free *R*-factor flags from the OppA−KAK data were added to the OppA−KK data so that the final free *R*-factors could be compared. The ligand and solvent molecules were also removed from the starting model. Refinement was carried out using REFMAC (Murshudov *et al*., 1997), and waters were added using X-Solvate (Oldfield, 1996a). Throughout the procedure individual atomic isotropic temperature factors were refined. Refinement statistics and model parameters are shown in Table 1.

Molecular Replacement. The unliganded OppA structure was solved by molecular replacement using the AMoRe package (Navaza, 1994). The coordinates of the 1.4 Å OppA−trilysine structure (PDB code 2olb) formed the basis of the starting model. OppA consists of three domains, two of which (domains I and II) are closely associated so that the structure is bilobate, in common with other periplasmic binding proteins. It could easily be seen from the earlier structures of closed, liganded OppA that the polypeptide segments connecting the two lobes could act as a flexible hinge. Two molecular replacement searches were therefore carried out, one with each lobe of the protein. Search fragment 1 contained domains I and II (residues 1−267 and 488−517), and search fragment 2 contained domain III (residues 271−484). Residues believed to be involved in the hinge motion were left out of the search models (residues 268−270 and 485−487). The ligand and all solvent molecules were also removed. Each of the two search fragments was placed in a *P*1 unit cell of dimensions $a = b = c = 75$ Å, $\alpha = \beta = \gamma = 90°$, and a cross-rotation function was calculated using each search fragment individually.

Six solutions were listed for the rotation search with fragment 1, of which the highest was 6σ above the mean with the next highest at 4σ above the mean. These rotation function solutions were used for calculation of the translation function. This was carried out in both $P3_121$ and $P3_221$, showing the space group to be $P3_221$. One solution of the translation search with fragment 1 had a higher correlation coefficient (41.7%) and a lower *R*-factor (49.8%) than the rest. This solution peak, which had a height 7.5σ above the mean with the next highest at 5σ above the mean, was therefore fixed and used in the translation step of search fragment 2.

The cross-rotation function of search fragment 2 generated no clear solution. The top 14 solutions produced by this rotation search (which clustered at heights between 3σ and 4σ above the mean) were used for the calculation of the translation function together with the fixed solution of search fragment 1. One solution was obtained with a high correlation coefficient (63.9%) and a low *R*-factor (39.4%) at 27σ above the mean with the next solution peak only 20% of this height. Ten cycles of rigid body refinement were carried out on the final solution, leading to an improvement in the correlation coefficient (75.9%) and a reduction in the *R*-factor (34.5%) with only minimal shifts in the molecular replacement parameters.

Refinement of the Unliganded OppA Structure. The molecular replacement model of the unliganded structure was refined by least squares minimization methods using the program PROLSQ (CCP4, 1994). The hinge residues 268−270 and 485−487, removed for molecular replacement, were built into clearly defined sections of $2F_o - F_c$ electron density maps before the start of refinement. Difference Fourier maps calculated with coefficients $2F_o - F_c$ and $F_o - F_c$ and phases derived from the model obtained after eight cycles of refinement were used to correct the model in X-FIT (Oldfield, 1996a). Forty water molecules were added at this stage using the automatic refinement program ARP (Lamzin & Wilson, 1993), and refinement was continued using the maximum likelihood refinement program REFMAC (Murshudov *et al.*, 1997). The bulk solvent correction in REFMAC was included. Individual atomic temperature factor refinement was introduced at this stage. Subsequently, the chain was checked and manually corrected by examination of the electron density maps, and remaining waters were added manually using the X-Solvate routine in QUANTA.

The crystal structures have been deposited in the Brookhaven Protein Data Bank.

Isothermal Titration Calorimetry. Experiments were carried out using an OMEGA titration microcalorimeter (MicroCal Inc., Northampton, MA). Details of the experimental setup are described elsewhere (Wiseman *et al.*, 1989). Fully degassed protein and peptide solutions in 50 mM Na^+/K^+ phosphate buffer at pH 7.0 were used. Protein was placed in the reaction cell (volume 1.36 mL), and the reference cell was filled with 0.01% sodium azide solution. Typically, 16 injections (15 μL) of peptide were made at intervals of 240 s. The syringe was stirred at a speed of 400 rpm to ensure rapid mixing in the cell. Experiments were carried out at 25 ± 0.2 °C. Concentrations of OppA between 0.01 and 0.13 mM were used in experiments to give *c* values ($c = [\text{OppA}]K_B$) of approximately 15. Heats of dilution were recorded in separate titration experiments as well as after saturation of the protein with peptide in all experiments.

ORIGIN software provided with the instrument was used to integrate the data, to plot the titration curves, and to fit these curves using nonlinear regression analysis for a single binding site. This procedure yields the equilibrium dissociation constant, K_D, and enthalpy change, ΔH, for the binding reaction. A typical trace measuring the binding of KKKA to OppA at 25 °C and pH 7.0 is shown in Figure 1.

RESULTS

Structure of the OppA−KK Complex. The overall structure of the OppA−KK complex is identical to that of a series of OppA−peptide complexes solved previously. Following least squares superposition of the Cα atoms of residues 10 to 510 from the refined structure onto the corresponding residues of the OppA−KAK starting model, the RMS deviation in main chain atomic positions is 0.39 Å. This value is typical of the differences observed in comparisons of a series of OppA complexes with tripeptide ligands (Tame *et al*., 1996).

Dipeptide Binding. Figure 2A shows electron density associated with the dilysine ligand and the surrounding protein residues. The ligand main chain is very well ordered in the binding site, and all of its polar atoms are engaged in hydrogen bonds or salt bridges. Thus, the α-amino group forms a salt bridge with the side chain carboxylate of Asp^{419} and potential charge−dipole interactions with the main chain carbonyl oxygen of Cys^{417} and the phenolic hydroxyl of Tyr^{109}. There also exists the possibility of favorable interac-

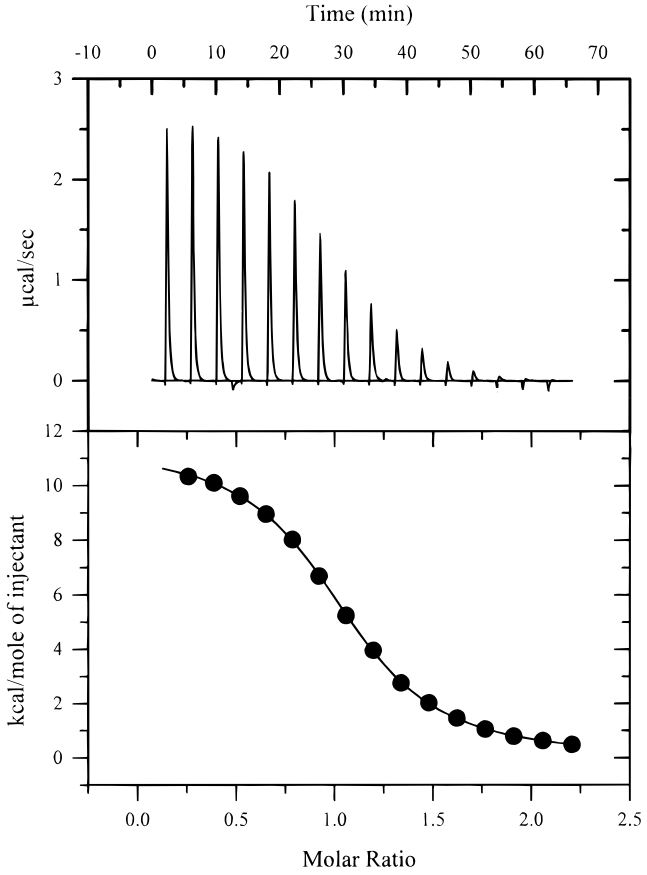

FIGURE 1: Isothermal titration calorimetry trace monitoring the binding of the peptide KKKA to OppA. The upper graph shows the heat taken up by the protein sample upon injection of ligand. The trace shows the power which must be supplied to a heating coil to maintain thermal equilibrium between the sample cell and the reference cell. The lower graph is a plot of heat absorbed on injection against molar ratio of ligand to protein.

tions between the peptide α-amino group and the π-electron cloud of the nearby Trp[416] (Figure 2B). The carbonyl and amino groups of the ligand's peptide bond are hydrogen bonded to the main chain amide and carbonyl groups of Cys[417] and Glu[32], respectively. The carboxylate oxygens of lysine-2 make extensive hydrogen-bonding interactions as shown in Figure 3A. Two well-defined water molecules (Wat[82] and Wat[197]), situated 2.7 and 2.8 Å, respectively, from the first of the carboxylate oxygens, appear to be important in dissipating the charge on the peptide's α-carboxylate group by mediating interactions with nearby arginine side chains (Figure 3A). Wat[82] forms a bridging interaction to NH1 of Arg[404] (O to N distance = 3.0 Å) while Wat[197] is situated 3.1 Å from NH1 of Arg[413]. The second carboxylate oxygen appears to form a hydrogen bond to the main chain amide group of Val[34] (O to N distance = 3.0 Å).

Figures 3 and 4 present comparisons of the mode of binding of the dipeptide with those of tripeptide and tetrapeptide ligands in OppA, emphasizing the close overlap of the peptides after the main chain protein atoms have been superimposed by least squares minimization. The interactions of the ligands' α-amino groups serve to anchor the peptides in the binding site, so that variations in peptide length are accommodated by alternative handling of the carboxy-terminal residues. The conserved interactions of the ligands' N-termini correspond well with the earlier genetic studies of Payne and Gilvarg (1968), who noted that a positively charged amino terminus on peptide substrates is a prerequisite for transport into the cell. The C-terminal carboxylate groups of the tri- and tetrapeptides form salt bridges with the charged side chains of Arg[413] and His[371], respectively. In the structure of the OppA−KKK complex, an acetate ion was found in the binding pocket, forming a salt bridge with His[371]. The position of this acetate ion corresponds closely to that of the C-terminal carboxylate of KKKA in the OppA−tetrapeptide complex. A second acetate ion was also apparent in close proximity to the Lys[307] ϵ-NH_3^+ group in the OppA−KKK structure, and so it seems likely that the carboxylate of a pentapeptide ligand also forms an ion pair interaction with a positively charged side chain in the protein (Tame *et al.*, 1995).

The use of water molecules to mediate interactions between the ligand C-terminus and the protein therefore appears to be found only for dipeptides. The flexibility of Gly[415] may be important for peptide binding. Its carbonyl oxygen forms a hydrogen bond to the amide nitrogen (O to N distance ~2.9 Å) of the peptide bond connecting ligand residues 2 and 3 in the tripeptide and tetrapeptide complexes (Figure 3B). The ϕ and ψ angles of Gly[415] change from −146° to −137° and 152° to 138° in the structures of OppA with dipeptide and tripeptide bound, respectively. This ϕ angle rotation of 9° and ψ angle change of 14° allow the carbonyl oxygen, which would otherwise be situated 3.1 Å from the first of the dipeptide's carboxy-terminal oxygens, to move away (to 3.6 Å) and avoid an unfavorable charge−dipole interaction. The conformation of Arg[413] is also altered significantly so that its side chain extends further toward the C-terminus of the dipeptide (Figure 3C).

The side chains of the two lysine residues are accommodated in much the same way as the corresponding side chains in the KKK and KKKA complexes (Tame *et al.*, 1995) (Figure 4). There is evidence of some disorder at lysine-2, particularly of the C_ϵ and N_ζ atoms, although only a single conformation has been modeled owing to the limited resolution of the diffraction data**.** This apparent disorder may correlate with the discrete disorder in the side chain of Glu[32]. Glu[32] forms a significant surface of the second side chain binding pocket in OppA and is observed to adopt either of two alternative conformations in a set of OppA−tripeptide complexes whose crystal structures have been determined (Tame *et al.*, 1996). In both conformations the carboxylate of Glu[32] makes an ion pair interaction with the imidazolium group of His[405]. In the dipeptide complex, the electron density maps suggest that both conformers are present, and these have been modeled with occupancies of 0.7 and 0.3 (Figure 5). The respective solvent molecules, Wat[173] and Wat[86], have also been modeled with partial occupancies according to the Glu[32] conformation.

The third side chain binding pocket, which is not occupied by ligand atoms in the dipeptide complex, is filled with water molecules, most of which are well ordered with temperature factors below the mean *B*-value for solvent atoms (Figure 3A). These waters form an extensive set of hydrogen bonds among themselves and with the surrounding side chains of Asn[246], Asn[247], Tyr[269], and Tyr[485]. Relative to the tripeptide complexes with lysine at position 3 there are some very small but distinct movements of protein side chains, including a rotation of the phenolic group of Tyr[485] (whose hydroxyl group is hydrogen bonded to Arg[413]) toward Val[34], resulting a slight narrowing of the pocket (Figure 3C).

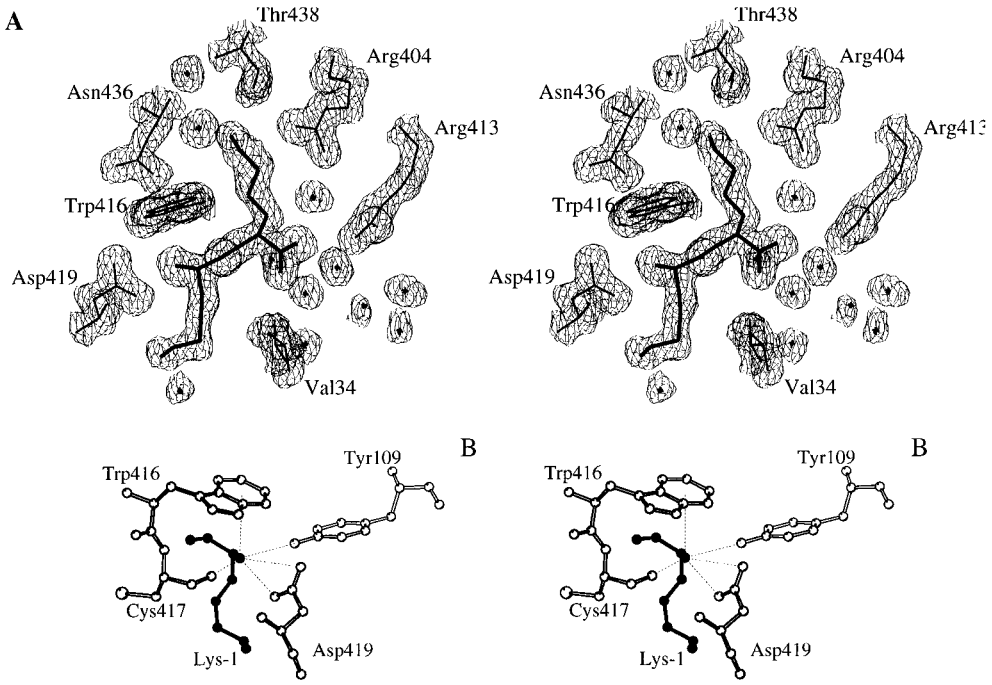

FIGURE 2: (A) Stereoview of the $2F_o - F_c$ electron density map contoured at 1σ in the binding pocket of the refined OppA−KK complex. The ligand, drawn in bold lines, is clearly defined in the density. Surrounding protein residues (thin lines) are labeled. (B) Stereoview of the interactions between the α-amino group of the dilysine ligand (filled lines) and OppA. Putative hydrogen bonding and electrostatic interactions are indicated by dashed lines.

Isothermal Titration Calorimetry. The affinity and enthalpy changes of ligand binding to OppA were measured by isothermal titration calorimetry (Table 2). As expected, no measurable binding takes place upon addition of the free amino acid lysine, consistent with earlier findings that the oligopeptide permease does not handle amino acids, which have their own set of transporters. The affinity of OppA for lysyllysine is ~60-fold lower than its affinity for the tripeptide and the tetrapeptide. Again, this observation is consistent with the equilibrium dialysis measurements of Guyer *et al.* (1986), who observed that dipeptides competed poorly with tripeptides for binding to OppA, and the fact that amino acid auxotrophs grow somewhat more slowly on dipeptide substrates containing the required amino acid than they do on corresponding tri- and tetrapeptides (Payne, 1968). The affinities of OppA for KKK and KKKA lie within the range of dissociation constants, 0.10−10 μM, normally observed for the binding of target ligands to periplasmic receptor proteins (Miller *et al.*, 1983).

Closer examination of the data shows that the favorable free energy of binding results from a dominant favorable entropy term which overcomes an unfavorable enthalpy of binding for all the ligands tested. Moreover, the modest changes in ΔG (~10 kJ·mol^{-1}) on replacing the dipeptide with a tetrapeptide result from larger but partially compensating changes in the ΔH (~35 kJ.mol^{-1}) and $T\Delta S$ (~45 kJ·mol^{-1}) terms. Increasing the length of the peptide is associated with more positive enthalpies and entropies of binding.

Structure of Unliganded OppA. The liganded and unliganded forms of OppA are related by a simple rigid-body rotation of domains I and II with respect to domain III, as was apparent from the molecular replacement solutions and anticipated from the closed, liganded structure. The three-dimensional structures of the individual domains are unaltered, as has been seen for the open and closedforms of DppA (Table 4).

The angle of opening in unliganded OppA calculated by determination of the rotation required to superimpose the two lobes of the protein in the unliganded form is 26°. This is a considerably smaller angle of opening than observed in other binding proteins for which the structures of the open, unliganded and closed, liganded forms have been determined. For example, the change in the hinge angle of maltodextrin binding protein (MBP) is 34°; those for lysine/arginine/ornithine binding protein, glutamine binding protein, and the dipeptide binding protein are 52°, 48°, and 55°, respectively (Sharff *et al.*, 1992; Oh *et al.*, 1993; Hsiao *et al.*, 1996; Dunten & Mowbray, 1995; Nickitenko *et al.*, 1995). In addition, the hinge motions for leucine/isoleucine/valine binding protein for which the structure of the open form alone is known have been estimated from molecular modeling calculations to be 30° (Sack *et al.*, 1989). In lactoferrin, which is closely related in structure to the periplasmic substrate binding proteins, the corresponding angle of opening is 53° (Baker & Lindley, 1992; Gerstein *et al.*, 1994). There is no obvious sequence or structural conservation among the binding proteins at the hinge region, although the transferrins do show a number of conserved residues and prolines are found in the hinge segments of many binding proteins. OppA has remarkably short crossover regions between domains I and III, consisting of residues 268−270 in one connection and residues 485 and 486 in the other, with adjacent residues forming part of the β-sheets in the two domains.

Where open and closed structures are known, the dramatic conformational changes that are observed can be attributed to large changes in the ϕ and ψ angles of just a small number of residues located in two segments of the polypeptide chain linking the two domains. In MBP, significant changes in the ϕ and/or ψ angles of a single residue in each of the two connecting segments account for the overall hinge motion,

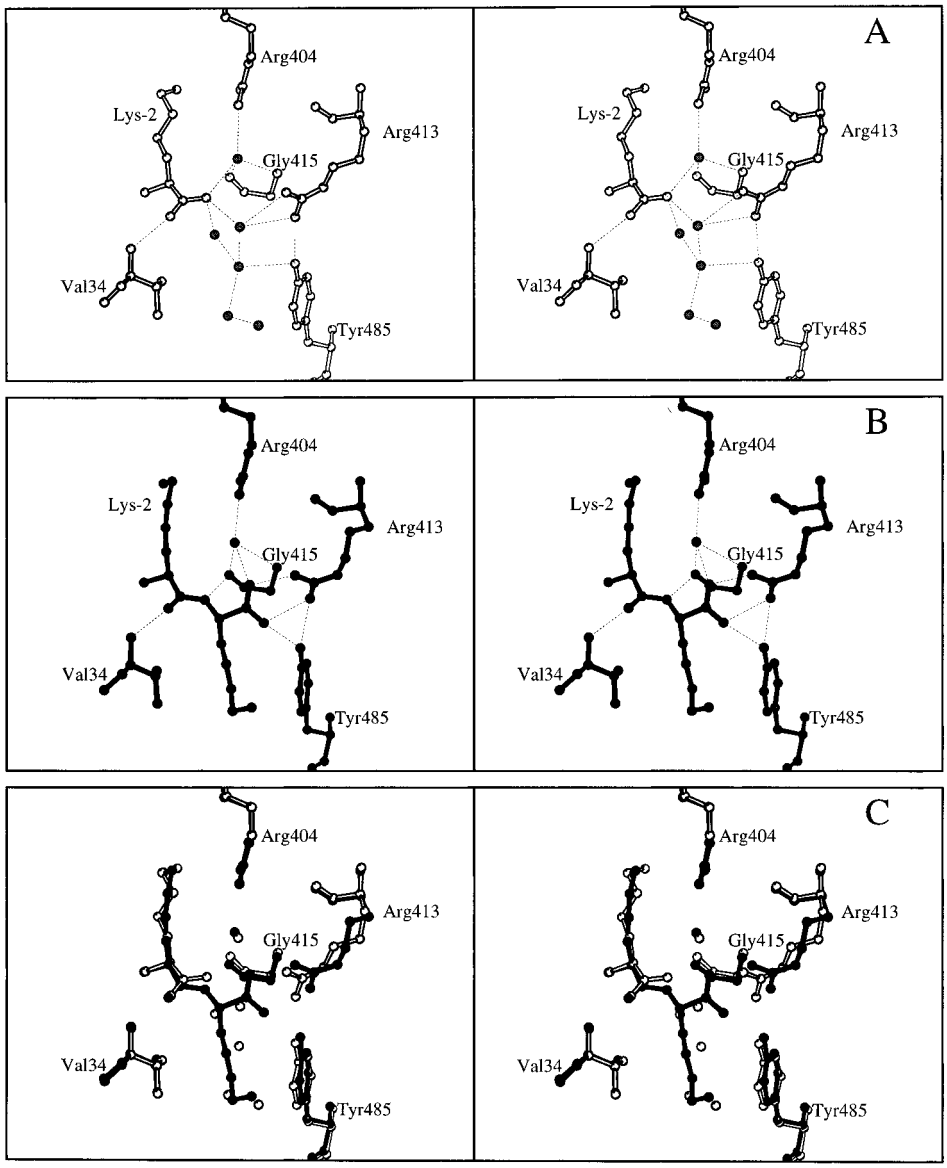

FIGURE 3: Stereoviews illustrating the binding of the C-termini of dilysine and trilysine ligands to OppA. (A) Lysine-2 of the dipeptide ligand with adjacent protein residues and water molecules (shaded). Note that waters at the base of pocket 3 form additional hydrogen bonds to the side chains of Asn^{246}, Asn^{247}, Tyr^{269}, and Tyr^{485}. (B) Lysine-2 and lysine-3 of the tripeptide ligand with surrounding protein atoms and water molecules. Potential hydrogen-bonding interactions are indicated by the dashed lines. (C) Comparison of the mode of binding of the C-terminal residues in the dipeptide and tripeptide complexes. The two structures are overlapped following least squares minimization of the positional displacements of the main chain Cα atoms of residues 10−510 of OppA. This diagram was produced using MOLSCRIPT (Kraulis, 1991).

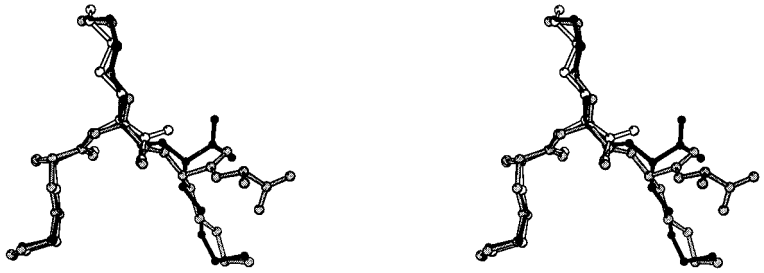

FIGURE 4: Overlap of the ligands in the complexes of OppA with KK (blank), KKK (filled), and KKKA (shaded). The three structures were superposed using least squares minimization procedures fitting the main chain Cα atoms of residues 10−510. The close superposition of the ligand atoms at their N-termini is apparent. This diagram was produced using MOLSCRIPT (Kraulis, 1991).

while in LAOBP the changes in ϕ/ψ angles which describe the hinge opening are distributed over three and four residues on the two connecting segments (Sharff *et al.*, 1992; Oh *et al.*, 1993). In DppA, large changes in ϕ angles of 43° and 42° at residues 262 and 478, respectively, and smaller but significant changes in adjacent torsion angles account for the relative domain motion. The equivalent residues in OppA (270 and 485) are also responsible for the opening, as shown in Table 3 and Figure 6. Interestingly, the hinge region includes Tyr^{485}, whose ω angle changes from 171°,

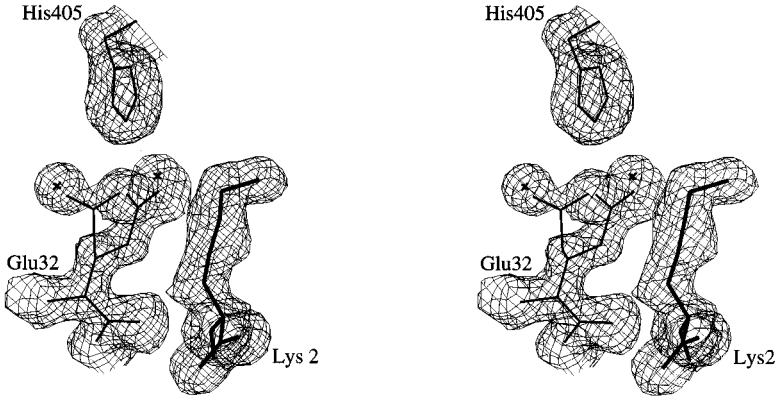

FIGURE 5: Stereoview of the electron density contoured at 1σ around the lysine-2 side chain and the adjacent protein residues Glu[32] and His[405]. The discrete disordering of the glutamate side chain is evident in the maps and becomes more apparent at lower σ levels. In the model the right and the left glutamate side chain conformers have been refined at occupancies of 0.7 and 0.3, respectively. The associated water molecule exchanges its position accordingly. In both conformers the electrostatic interactions with the His[405] imidazole are maintained with Glu[32]Oϵ to His[405]Nϵ distances of 2.7 and 2.8 Å, respectively.

Table 2: Isothermal Titration Calorimetry Data for the Binding of Peptides to OppA at pH 7.0 and 25 °C

peptide	$K_D \times 10^6$ (M)	ΔH (kJ·mol^{-1})	ΔG (kJ·mol^{-1})	$T\Delta S$ (kJ·mol^{-1})
K	nd	nd	nd	nd
KK	125 ± 16	12.8 ± 1.3	−22.1 ± 0.4	34.9 ± 1.8
KKK	1.96 ± 0.38	27.3 ± 6.7	−32.6 ± 0.5	62.6 ± 7.1
KKKA	2.70 ± 0.51	47.4 ± 0.4	−31.8 ± 1.1	79.3 ± 1.5

[a] The values given were derived from two titrations for KKK and KKKA and one titration for KK. Values of K_D and ΔH for KKK and KKKA are weighted averages of the measured values from the two experiments. nd = not detectable.

Table 3: Changes in ϕ and ψ Angles of Hinge Residues of OppA and DppA upon Opening

OppA[a]			DppA		
residue no.	ΔΦ	ΔΨ	residue no.	ΔΦ	ΔΨ
270	9	−9	262	43	4
271	0	−5	263	−18	4
272	4	−4	264	−13	−10
273	6	−14	265	15	0
484	9	2	477	−16	14
485	19	−14	478	42	15
486	7	−4	479	−24	−16

[a] The root mean squared deviation in ϕ and ψ angle changes between the liganded and unliganded OppA forms is 6.6° and 6.7° respectively.

which is itself a low ω angle in the liganded structures, to 167° in the unliganded form. Large deviations from the mean ω angle of 179.5° have been noted (MacArthur & Thornton, 1996; Sevcik *et al.*, 1996).

Figure 7 shows space-filling representations of liganded OppA, unliganded OppA, and unliganded OppA into which the trilysine ligand has been fitted. The figure illustrates that the ligand would be sterically restricted in its approach to the binding site if the extent of hinge opening were limited to 26° in solution. The observed angle of opening is almost certainly governed by crystal packing. The 30° range of hinge-opening angles observed among the binding proteins and the absence of any correlation between the extent of opening and the size of the cognate ligands, support the suggestion that the unliganded form of the binding proteins is best described as an ensemble of "open" structures in rapid equilibrium with one another and indeed with the unliganded closed form (Miller *et al.*, 1983; Flocco & Mowbray, 1994).

Comparisons of the overall structures of liganded and unliganded OppA are shown in Table 4 and Figure 8. The largest displacements are of loops on the surface of the protein, many of which bind uranium ions in the liganded structures. Uranyl acetate is essential for crystallization, and the heavy metal ions mediate a number of intermolecular interactions in the lattice which undoubtedly contribute to the high resolution of the X-ray scattering by the $P2_12_12_1$ crystal form.

Solvent Structure. A large number of water molecules are trapped in the protein upon ligand binding, many of which are important in adapting the cavity in OppA to accommodate side chains of diverse structure (Tame *et al.*, 1996). These water molecules fill the volume not occupied by the smaller ligands and mediate interactions between polar ligand atoms and the protein. A much smaller number of ordered water molecules are associated with the exposed cavity-forming residues of unliganded OppA (28 in the case of OppA−KAK and 13 in the unliganded protein). This is an inevitable consequence of the lower resolution of the diffraction data obtained from the crystals of the unliganded protein, although it may also be due in part to the different precipitants used for crystallization [poly(ethylene glycol) 4000 in the case of liganded OppA versus 3 M ammonium sulfate for unliganded OppA]. It is interesting to note, however, that significantly fewer ordered water molecules were observed on the exposed, cavity-forming surfaces of open unliganded MBP (21) than were observed buried in the substrate binding cavity of the MBP−maltose complex (35), even though the respective crystals diffract to comparable resolution and both were crystallized using poly(ethylene glycol) (Sharff *et al.*, 1992).

Of the ordered waters which are bound in the exposed cavity of unliganded OppA, seven cluster in the pocket that normally accommodates the second ligand side chain. The arrangement of these solvent molecules is illustrated in Figure 9 which shows a superposition of the structures of unliganded OppA and OppA complexed with dilysine and with trilysine. It is evident that five of the six water molecules surrounding the lysine-2 side chains in the complexes are retained in the unliganded structure; moreover, the positions of these solvent molecules are closely "conserved", despite the differences in the crystallization conditions (particularly the pH and ionic

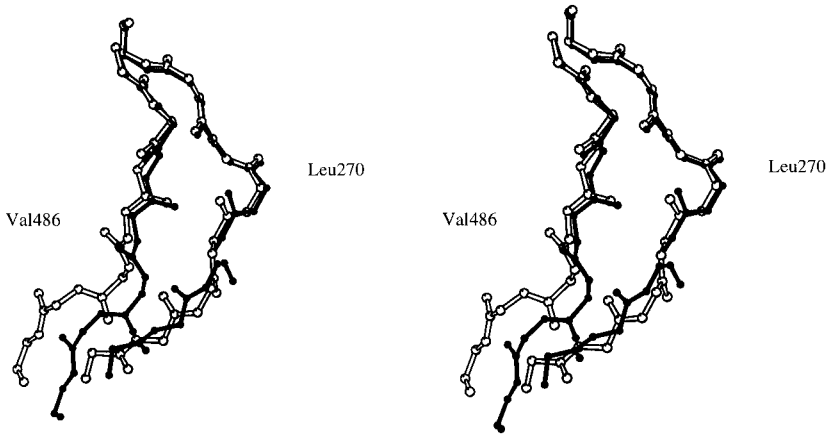

FIGURE 6: Stereo diagram showing the hinge regions of the liganded and unliganded OppA structures between residues 262−273 and 480−489 clearly demonstrating the movement at the hinge. Structures are superposed on the Cα atoms of their third domains (between residues 270 and 480). This diagram was produced using MOLSCRIPT (Kraulis, 1991).

strength) and the methods of refinement used. Glu[32], with which the sixth water molecule is associated, has moved away from His[405] as the lobes of the protein separate. Two further well-ordered solvent molecules are observed in the unliganded protein. These waters occupy the volume taken up by the lysine-2 side chain and are displaced by peptide ligands containing large residues at position 2; however, they are retained in complexes with peptides containing alanine or glycine at position 2 (Tame *et al.*, 1996; S.H.S., unpublished observations).

Conserved waters in the ligand binding cavity have also been noted in the liganded and unliganded forms of MBP. Eight wholly or partially conserved water molecules are distributed over both surfaces exposed in the open form, only one of which is involved in hydrogen bonding to the ligand in the closed, liganded protein (Sharff *et al.*, 1992). Conserved water molecules have also been noted in the open, unliganded and closed, liganded forms of LAOBP. Two of these water molecules play an important role in adapting the side chain pocket to accommodate the basic side chains of lysine, arginine, or ornithine (Oh *et al.*, 1994).

DISCUSSION

Unliganded versus Liganded OppA. A primary reason for our determination of the crystal structure of OppA in the unliganded form was in an attempt to establish a function for domain II in OppA. The greater size of OppA, M_r = 58 808, relative to the majority of the binding proteins whose structures have been determined to date and whose relative molecular masses cluster in the range 26 000−41 000 can be attributed to an insertion of residues 45−168 which form the extra domain. This extra sequence is well conserved among a subset of periplasmic receptor proteins including those for dipeptides and nickel (Tam & Saier, 1993).

The unliganded OppA crystal structure illustrates clearly that there is no motion of domain I relative to domain II. Nickitenko *et al.* (1995) have determined the crystal structure of unliganded DppA and compared its domain topology with that of liganded OppA and made the same observation. This conclusion is confirmed by direct comparison of the liganded and unliganded forms of DppA (Nickitenko *et al.*, 1995; Dunten & Mowbray, 1995). Nickitenko *et al.* refer to domains I and II as subdomains Ia and Ib on the basis of their earlier analysis of the structure of maltodextrin binding protein where a subdomain serves to extend the ligand binding groove so that larger sugars may be accommodated (Spurlino *et al.*, 1991). The more substantial third domain (or subdomain) in OppA does not appear to serve this function since the longer peptides extend away from domain II. The pocket that accepts the side chain of the first ligand residue is, however, closed off in part by residues Tyr[109], His[161], and Pro[162] of domain II.

The similarities in the structure and mechanism of ligand binding in the periplasmic substrate binding proteins imply a common mode of interaction with the membrane components of their respective transporters. It is generally accepted that the unliganded proteins are in a dynamic equilibrium between open and closed states. It should be emphasized again that the extent of domain opening seen in the crystal structures of the open forms is probably governed by crystal packing interactions. In solution it is likely that a population of open forms exist with fluctuations in the extent of domain opening. The ligand then associates initially with one of the two lobes in the open form, the second lobe closes over the ligand, and interactions between the ligand and the second lobe then serve to stabilize the closed form of the protein. In all the liganded structures examined, including OppA, the ligand makes more extensive contacts with one of the lobes than it does with the other. Moreover, leucine soaked into open, unliganded LIVBP crystals was observed to bind exclusively to the N-domain (Sack *et al.*, 1989). The closed form of the proteins has an external surface quite distinct from that of the open form, and it is proposed that this form is preferentially recognized by the less abundant membrane components. The available evidence indicates that the residues which mediate interactions with the membrane components cluster in patches on both lobes of the binding protein so that they are brought into appropriate juxtaposition only in the closed form (Prossnitz *et al.*, 1988). It is believed that the binding proteins interact with the exterior surfaces of both the membrane-spanning components.

In the case of OppA and DppA, which bind an array of ligands of quite different size, shape, and charge, the enclosure of the ligand in the protein interior has the additional special feature of masking differences among the ligands. The external appearance of the closed, liganded protein is similar, regardless of the ligand that has been enclosed. This property allows peptide-based antibiotics,

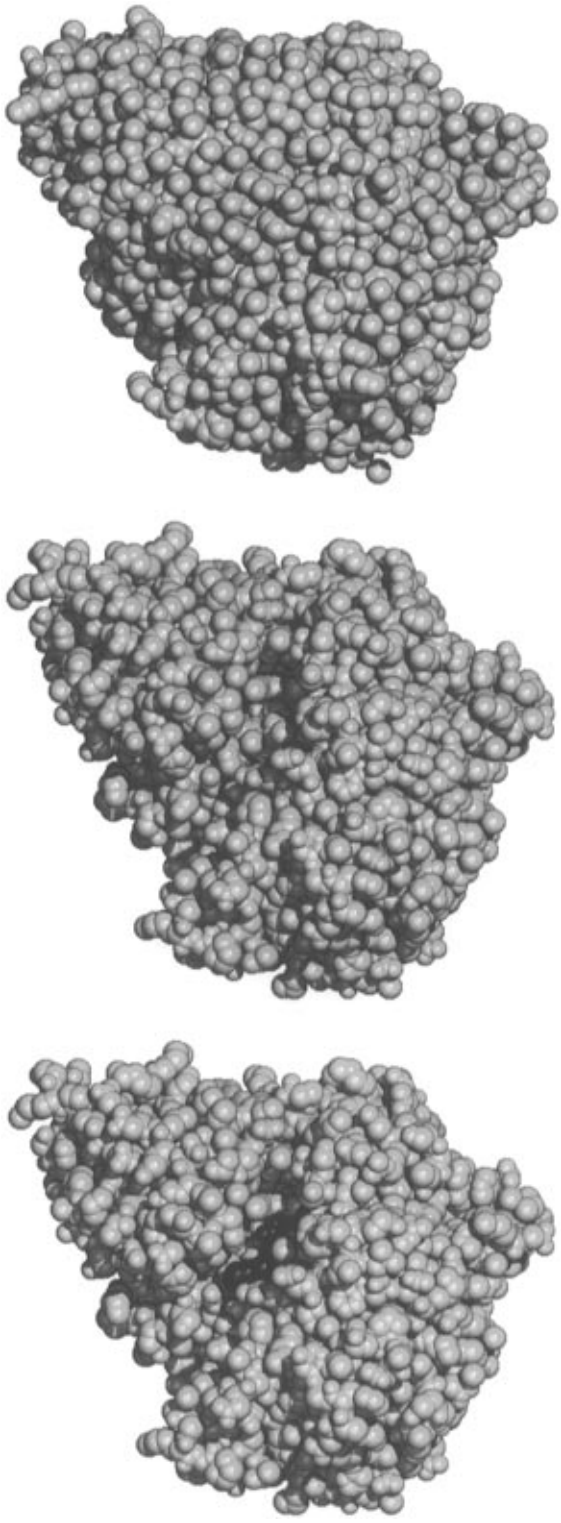

FIGURE 7: Space-filling diagrams of (A, top) liganded OppA, (B, middle) unliganded OppA, and (C, bottom) unliganded OppA onto which the trilysine ligand from the OppA−KKK complex has been superposed. The KKK ligand from the OppA−KKK complex was positioned in the figure by application of the matrix which minimizes the least squares displacements of the Cα atoms of residues 270−480 in the OppA−KKK from the corresponding atoms in the unliganded protein. In (A) and (C) the ligand is colored in red. The figure emphasizes the complete engulfment of the ligand in the closed form of the protein so that no ligand atoms are visible in (A) as well as the incomplete exposure of the binding cleft in the open form (C).

which bind to OppA, to be transported into the cell with OppA acting, in a sense, as a Trojan horse (Hammond *et al*., 1987; Higgins 1987; J. R. H. Tame, unpublished observations).

Dipeptide Binding in DppA and OppA. The domain organization and the polypeptide chain topology of OppA and DppA are substantially the same, as shown in Table 4. In their comparison of the structure of unliganded DppA with liganded OppA, Nickitenko *et al*. (1995) noted nine segments of the polypeptide whose conformations differ significantly between the two proteins. Of these, eight lie on the surface of the molecule, and most of these include insertions or deletions of residues in loops connecting elements of secondary structure. The ninth segment is located in the peptide binding site and includes a loop which in DppA contains five extra residues. In the complex of DppA with Gly-Leu, this loop reaches into the binding cavity, apparently preventing the binding of ligands larger than dipeptides (Dunten & Mowbray, 1995). The side chains of two residues, Arg^{355} and Tyr^{357}, are in close proximity to the C-terminus of the bound dipeptide and probably form ion-pairing and charge−dipole interactions, respectively, with its α-carboxylate group. Otherwise, the interactions between the main chain functional groups of the dipeptide Gly-Leu and residues lining the cavity in DppA are very similar to those made by lysyllysine bound in OppA.

OppA's affinity for the dipeptide is significantly lower than that which periplasmic receptor proteins usually exhibit toward their cognate ligands. The preferred receptor for extracellular dipeptides is presumably DppA, since this protein is a mediator not only of dipeptide transport but also of dipeptide chemotaxis (Manson *et al.*, 1986). It is conceivable that tight binding of dipeptides by OppA, which does not elicit chemotaxis, would be disadvantageous to the cell. Nevertheless, Opp can handle dipeptides, and this may assist survival of Dpp^- mutants under stringent growth conditions. It may also allow different systems to work together when ligand concentrations are high. This multiple coverage is common among these systems.

Structure−Affinity Considerations. As shown in Table 2, the affinity of OppA for lysyllysine is ∼60-fold lower than its affinity for the longer lysine-containing peptides corresponding to a $\Delta\Delta G$ of ∼10 kJ·mol^{-1}. Comparing the dipeptide and the tripeptide complexes, the principal structural differences are as follows: (i) the α-CO_2^- groups are handled in different ways (direct ion pairing *versus* water-mediated ion pairing), (ii) the protein forms additional interactions with the main chain of the ligand in the tripeptide complex, including hydrogen bonding of the polar peptide linkage between residues 2 and 3, (iii) there are additional interactions with the side chain of residue 3 that include contacts to the aliphatic portion of the lysine 3 side chain and direct/water-mediated polar interactions with its charged ε-amino group, and (iv) additional ordered water molecules are buried in the dipeptide complex—these make extensive hydrogen-bonding interactions with polar protein groups and with each other. With the exception of (i), qualitatively similar structural differences emerge from comparison of the tripeptide and tetrapeptide complexes, even though the affinities are very similar as shown in Table 2.

Table 2 emphasizes that the enthalpy and entropy changes accompanying ligand binding vary more widely than the changes in ΔG. For all three ligands, binding is entropy driven and there is no correlation between the enthalpy and the free energy changes accompanying binding; this lack of

Table 4: Root Mean Squared Displacements (in Å) of Cα Atoms in Individual Domains between Open and Closed Forms of OppA and DppA

domain[a]	liganded and unliganded OppA structures	liganded and unliganded DppA structures	liganded OppA and liganded DppA structures[b]	unliganded OppA and unliganded DppA structures[b]
I	0.50	0.47	1.1 (114)	1.2 (115)
II	0.49	0.54	0.9 (64)	1.1 (67)
III	0.54	0.57	1.1 (144)	1.2 (141)

[a] Domain numbering is as follows: OppA, domain I residues 1−44, 189−269, and 487−517; domain II residues 45−188; domain III residues 270−486; DppA, domain I residues 1−32, 183−262, and 479−507; domain II residues 33−182; domain III residues 263−478. This numbering differs slightly from that used previously (Tame *et al.*, 1994). The Brookhaven Protein Data Bank files used for the comparisons shown in this table are as follows: liganded OppA, 2olb.pdb; unliganded OppA, 1rkm.pdb; liganded DppA, 1dpp.pdb; unliganded DppA ,1dpe.pdb. [b] These structures were superposed on closest matching atoms only, as defined in QUANTA (1996). The number of atoms overlaid in each case is shown in parentheses.

FIGURE 8: Stereo ribbon diagrams of (A) unliganded OppA and (B) OppA−KKK (PDB identification code 2olb) with the trilysine ligand atoms displayed as spheres of appropriate van der Waals radii. The ligand binding cleft is seen to be exposed in the unliganded structure. This diagram was produced using MOLSCRIPT (Kraulis, 1991).

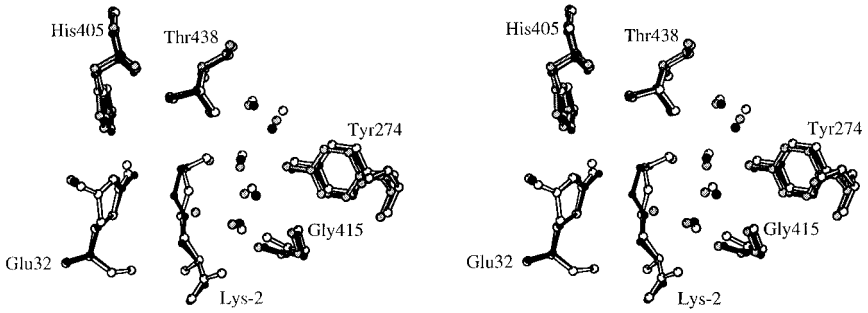

FIGURE 9: Stereo diagram showing superposed structures of unliganded OppA (shaded), OppA bound to KK (blank), and KKK (filled) in the region of the second side chain binding pocket. Structures were superposed using least squares minimization to overlap protein Cα atoms between residues 270 and 480. Water molecules associated with each of the structures are shaded correspondingly. Glu^{32} has moved away in the unliganded structure and is discretely disordered in the OppA−KK structure (Figure 5). This diagram was produced using MOLSCRIPT (Kraulis, 1991).

correlation is frequently encountered in processes involving proteins (Sturtevant, 1994). The weaker binding of the dipeptide is associated with a more favorable (less positive) ΔH term relative to the longer ligands, $\Delta\Delta H_{KKK\rightarrow KK} = -15$ kJ·mol^{-1}, which is more than offset by a poorer (less positive) ΔS term, $\Delta\Delta S_{KKK\rightarrow KK} = \sim -100$ J·K^{-1}·mol^{-1}. Similarly, the closely matching affinities that OppA exhibits toward the tripeptide and tetrapeptide ligands, $\Delta\Delta G_{KKKA\rightarrow KKK} = -0.8$ kJ·mol^{-1}, disguise large differences in the enthalpy and entropy of binding, $\Delta\Delta H_{KKKA\rightarrow KKK} = -20$ kJ·mol^{-1} and

$\Delta\Delta S_{KKKA\rightarrow KKK} = \sim -60$ J·K^{-1}·mol^{-1}. Thus, the sum of the changes in noncovalent interaction energies upon complex formation (ΔH) is most favorable for shorter ligands, for these ligands however, the increase in the disorder of the system ΔS is smaller.

The dipeptide's carboxylate group forms charge−dipole interactions with water molecules which themselves participate in similar interactions with the positively charged side chains of Arg^{404} and Arg^{413}. These water-mediated interactions contrast with the direct ion-pairing interactions of the carboxylate groups of the tripeptide and the tetrapeptide ligands with Arg^{413} and His^{307}, respectively. A similar mode of binding of the carboxylate group is observed in the binding of dipeptides by the dipeptide binding protein (DppA), where the Arg^{355} side chain forms a direct ion pair with the carboxylate group of Gly-Leu (Dunten & Mowbray, 1995). There is a therefore a correlation between high-affinity peptide binding (lower ΔG) and direct ion pairing of the peptide's α-carboxylate group. Water-bridged ion pairs are expected to interact more weakly and contribute less to the enthalpy of binding than a pair of ions in direct contact with one another. However, as the observed $\Delta\Delta H_{(KKK\rightarrow KK)}$ is negative, other favorable enthalpic contributions must more than compensate.

These will include the bonding interactions of the five water molecules which are buried in the protein in complex with the dipeptide but displaced when the tripeptide is bound. These water molecules are well ordered and appear to make an extended set of strong hydrogen bonds among themselves and with polar protein and ligand groups in the vacant pocket 3 of the dipeptide complex. This favorable enthalpic contribution will be offset by hydrophobic interactions which favor binding of the tripeptide. Relative to the dipeptide, tripeptide binding leads to the burial of an additional 260 Å^2 of molecular surface area of which 172 Å^2 is nonpolar (Connolly, 1983). Displacement of water upon formation of additional nonpolar contacts between the protein and the ligand will give rise to closer packed surfaces and more favorable van der Waals interactions. However, the major thermodynamic contribution is expected to be the favorable entropy change accompanying displacement of these water molecules. The magnitude of this term is hard to estimate as it depends on the specific interactions that these water molecules are able to make in the cavity. Measurements based on waters of hydration of crystal salts suggest an entropic gain of 10−30 J·mol^{-1}·K^{-1}/water (Dunitz, 1994; Tame *et al*., 1996).

Similar considerations apply to the comparison of the binding of a tripeptide ligand with a tetrapeptide ligand. In this case, however, both ligands' carboxy termini form direct salt bridges with the protein, and only three additional water molecules are displaced in the tetrapeptide complex. An additional 149 Å^2 of surface area is buried in the tetrapeptide complex of which 107 Å^2 is nonpolar.

While accurate crystal structures of the liganded and, to a slightly lesser extent, the unliganded forms of the protein are known, the structure, dynamics, and solvation of the unbound peptides are unknown in these experiments. It may be that the differences in the enthalpy and entropy changes shown in Table 2 are significantly affected by conformational and solvation differences among the free ligands. Experiments on an extended series of peptides are underway to try to find clear correlations between the structures of the different OppA−ligand complexes and the thermodynamic parameters associated with complex formation.

ACKNOWLEDGMENT

We thank the BBSRC for beam time at the Synchrotron Radiation Source at Daresbury. We are grateful to J. Ladbury for advice on calorimetry and to J. Brannigan, G. Dodson, and J. Whittingham for helpful comments on the manuscript.

REFERENCES

Abouhamad, W. N., Manson, M., Gibson, M. M., & Higgins, C. F. (1991) *Mol. Microbiol. 5*, 1035−1047.
Ames, G. F.-L. (1986) *Annu. Rev. Biochem. 55*, 397−425.
Baker, E. N., & Lindley, P. F. (1992) *J. Inorg. Biochem. 47*, 147−160.
CCP4. Collaborative Computer Project Number 4 (1994) *Acta Crystallogr. D50*, 760−763.
Connolly, M. L. (1983) *Science 221*, 709−713.
Dunitz, J. D. (1994) *Science 264*, 670.
Dunten, P., & Mowbray, S. L. (1995) *Protein Sci. 4*, 2327−2334.
Flocco, M. M., & Mowbray, S. L. (1994) *J. Biol. Chem. 269*, 8931−8936.
Furlong, C. E. (1987) in *Cellular and Molecular Biology* (Neidhardt, F. C., Ed.) pp 768−796, American Society for Microbiology, Washington, DC.
Gerstein, M., Lesk, A. M., & Chothia, C. (1994) *Biochemistry 33*, 6739−6749.
Glover, I. D., Denny, R. C., Nguti, N. D., McSweeny, S. M., Kinder, S. H., Thompson, A. W., Dodson, E. J., Wilkinson, A. J., & Tame, J. R. H. (1995) *Acta Crystallogr. D51*, 39−47.
Guyer, C. A., Morgan, D. G., & Staros, J. V. (1986) *J. Bacteriol. 168*, 775−779.
Hammond, S. M., Claesson, A., Jansson, A. M., Larsson, L. G., Pring, B. G., Town, C. M., & Ekstrom, B. (1987) *Nature (London) 327*, 730−732.
Higgins, C. F. (1987) *Nature (London) 327*, 655−656.
Higgins, C. F. (1992) *Annu. Rev. Cell Biol. 8*, 67−113.
Higgins, C. F., Haag, P. D., Nikaido, K., Ardeshir, F., Garcia, G., & Ames, G. F.-L. (1982) *Nature (London) 298*, 723−727.
Hsiao, C.-D., Sun, Y.-J., Rose, J., & Wang, B. C. (1996) *J. Mol. Biol. 262*, 225−242.
Jacobson, B. L., & Quiocho, F. A. (1988) *J. Mol. Biol. 204*, 783−787.
Kraulis, P. (1991) *J. Appl. Crystallogr. 24*, 946−950.
Lamzin, V. S., & Wilson, K. S. (1993) *Acta Crystallogr. D49*, 129−147.
Luecke, H., & Quiocho, F. A. (1990) *Nature (London) 347*, 402−406.
MacArthur, M. W., & Thornton, J. M. (1996) *J. Mol. Biol. 264*, 1180−1195.
Manson, M. D., Blank, V., Brade, G., & Higgins, C. F. (1986) *Nature (London) 321*, 253−256.
Mao, B., Pear, M. R., McCammon, J. A., & Quiocho, F. A. (1982) *J. Biol. Chem. 257*, 1131−1133.
Miller, D. M., Olson, J. S., Pflugrath, J. W., & Quiocho, F. A. (1983) *J. Biol. Chem. 258*, 13665−13672.
Murshudov, G. N., Vagin, A. A., & Dodson, E. J. (1997) *Acta Crystallogr. D53*, 240−255.
Navaza, J. (1994) *Acta Crystallogr. A50*, 157−163.
Nickitenko, A. V., Trakhanov, S., & Quiocho, F. A. (1995) *Biochemistry 34*, 16585−16595.
Oh, B.-H., Pandit, J., Kang, C.-H., Nikaido, K., Gokcen, S., Ames, G. F.-L., & Kim, S.-H. (1993) *J. Biol. Chem. 268*, 11348−11355.
Oh, B.-H., Ames, G. F.-L., & Kim, S.-H. (1994) *J. Biol. Chem. 269*, 26323−26330.
Oldfield, T. J. (1996a) in *Macromolecular Refinement. Proceedings of the CCP4 Study Weekend*, 67−74, SRS Daresbury Laboratory, Warrington, U.K.
Otwinowski, Z. (1990) *DENZO Data Processing Package*, Yale University, New Haven, CT.
Payne, J. W. (1968) *J. Biol. Chem. 243*, 3395−3403.

Payne, J. W., & Gilvarg, C. (1968) *J. Biol. Chem. 243*, 6291−6299.

Prossnitz, E., Nikaido, K., Ulbrich, S. J., & Ames, G. F.-L. (1988) *J. Biol. Chem. 263*, 17917−17920.

QUANTA 96 beta release (1996) *User's Reference*, Molecular Simulations, San Diego.

Quiocho, F. A., & Vyas, N. K. (1984) *Nature (London) 310*, 381−386.

Quiocho, F. A., & Ledvina, P. S. (1996) *Mol. Microbiol. 20*, 17−25.

Quiocho, F. A., Wilson, D. K., & Vyas, N. K. (1989) *Nature (London) 340*, 404−407.

Sack, J. S., Trakhanov, S. D., Tsigannik, I. H., & Quiocho, F. A. (1989) *J. Mol. Biol. 206*, 193−207.

Sevcik, J., Dauter, Z., Lamzin, V. S., & Wilson, K. S. (1996) *Acta Crystallogr. D52*, 327−344.

Sharff, A. J., Rodseth, L. E., Spurlino, J. C., & Quiocho F. A. (1992) *Biochemistry 31*, 10657−10663.

Spurlino, J. C., Lu, G.-Y., & Quiocho, F. A. (1991) *J. Biol. Chem. 266*, 5202−5219.

Sturtevant, J. M. (1994) *Curr. Opin. Struct. Biol. 4*, 69−78.

Tam, R., & Saier, M. H. (1993) *Microbiol. Rev. 57*, 320−346.

Tame, J. R. H., Murshudov, G. N., Dodson, E. J., Neil, T. K., Dodson, G. G., Higgins, C. F., & Wilkinson, A. J. (1994) *Science 264*, 1578−1581.

Tame, J. R. H., Dodson, E. J., Murshudov, G. N., Higgins, C. F., & Wilkinson, A. J. (1995) *Structure 3*, 1395−1406.

Tame, J. R. H., Sleigh, S. H., Wilkinson, A. J., & Ladbury, J. E. (1996) *Nat. Struct. Biol. 3*, 998−1001.

Vyas, M. N., Vyas, N. K., & Quiocho, F. A. (1994) *Biochemistry 33*, 4762−4768.

Wilkinson, A. J. (1996) *Chem. Biol. 3*, 519−524.

Wiseman, T., Williston, S., Brandts, J. F., & Lin, L.-N. (1989) *Anal. Biochem. 179*, 131−137.

Yao, N., Trakhanov, S., & Quiocho, F. A. (1994) *Biochemistry 33*, 4769−4779.

BI970457U